Supplementary Materials for

Spectral Response Analysis: An Indirect and Non-Destructive Methodology for Biocrusts Chlorophyll Quantification

José Raúl Román, Emilio Rodríguez-Caballero, Borja Rodríguez-Lozano, Beatriz Roncero-Ramos, Sonia Chamizo, Pilar Águila-Carricondo and Yolanda Cantón

Table S1. Soil texture, pH, electrical conductivity, total organic carbon (TOC) and total nitrogen (TN) of the of the three soils employed in this study: Las Amoladeras, El Cautivo and Gádor quarry (from Román et al., 2018).

Soil types	Soil texture			pH	Electrical Conductivity (mS/cm)	TOC (g/Kg)	TN (g/Kg)
	Sand (%)	Silt (%)	Clay (%)				
Las Amoladeras	61.50 ± 5.10	28.40 ± 4.20	10.10 ± 2.10	8.03 ± 0.04	0.16 ± 0.01	21.41 ± 0.96	2.07 ± 0.11
El Cautivo	29.20 ± 5.40	58.60 ± 5.80	12.20 ± 4.20	8.28 ± 0.12	0.13 ± 0.01	3.87 ± 0.09	0.57 ± 0.04
Gádor quarry	31.20 ± 4.65	43.10 ± 2.34	25.70 ± 2.80	8.57 ± 0.03	1.98 ± 0.18	0.24 ± 0.21	0.17 ± 0.09

Table S2. Summary of the different spectral indices used in this study. R: reflectance; ϱ: the first derivative of reflectance; RBLUE: reflectance in the blue region, RGREEN: reflectance in the green region, RNIR: reflectance in near-infrared region.

Index	Formulation	Reference
Simple ratio or modified simple ratio of reflectance or derivatives		
YCAR	R_{600}/R_{680}	Schlemmer et al. (2005)
OCAR	R_{630}/R_{680}	Schlemmer et al. (2005)
Vogelman3	R_{740}/R_{720}	Vogelman et al. (1993)
SRPI (Simple Ratio Pigment Index)	R_{430}/R_{680}	Peñuelas et al. (1994)
Vogelman1	$\varrho_{715}/\varrho_{705}$	Vogelman et al. (1993)
dSR1*	$\varrho_{725}/\varrho_{702}$	Kochubey and Kazantsev (2007)
dSR2*	$\varrho_{705}/\varrho_{722}$	Zarco-Tejada et al. (2002)
Datt-CabCx+c	$R_{860}/(R_{550} * R_{708})$	Datt (1998)
PSRI	$(R_{680} - R_{500})/R_{750}$	Merzlyak et al. (1999)
mSR705	$(R_{750} - R_{445})/(R_{705} - R_{445})$	Sims and Gamon (2002)
BmSR	$(\varrho_{722} - \varrho_{502})/(\varrho_{700} - \varrho_{502})$	le Maire et al. (2004)

5 **Table S2 (Continuation)**

Index	Formulation	Reference
	Normalized difference of derivatives	
BND	$(\varrho_{722} - \varrho_{700})/(\varrho_{722} + \varrho_{700})$	le Maire et al. (2004)
	Modified normalized difference of derivatives	
BmND	$(\varrho_{722} - \varrho_{700})/(\varrho_{722} + \varrho_{700} - 2\varrho_{502})$	le Maire et al. (2004)
	Indices related with red edge derived with derivatives	
dRE	First derivative maxima in red-edge region (680-780 nm)	Filella and Peñuelas (1994)
∑dRE	Sum of first derivative reflectance in red-edge region (680-780 nm)	Filella and Peñuelas (1994)
EGFR (Ratio of first derivative maxima in red-edge region and green region (530-570 nm))	dRE/dG	Penuelas et al. (1994)
EGFN	(dRE − dG)/(dRE + dG)	Penuelas et al. (1994)
EBAR (Ratio of Sum of first derivative reflectance in red-edge region (680-780 nm) and blue region (490-530 nm))	∑dRE/∑dB	Xue et al. (2009)
EBAN	(∑dRE − ∑dB)/(∑dRE + ∑dB)	Xue et al. (2009)
EBFR	dRE/dB	Xue et al. (2009)
EBFN	(dRE − dB)/(dRE + dB)	Xue et al. (2009)

6 **Table S2 (Continuation)**

Index	Formulation	Reference
	Broad band indices	
Normalized Difference Vegetation Index(NDVI)	$(R_{NIR} - R_{RED} / R_{NIR} + R_{RED})$	Rouse et al. (1973)
Enhanced Vegetation Index (EVI)	$2.5 * (R_{NIR} - R_{RED}) / (R_{NIR} + 6R_{RED} - 7.5R_{BLUE} + 1)$	Huete et al. (2002)
Soil-adjusted vegetation index (SAVI)	$(R_{NIR} - R_{RED} / R_{NIR} + R_{RED} + 0.5) * (1+ 0.5)$	Huete (1988)
Optimized soil-adjusted vegetation index (OSAVI)	$(R_{NIR} - R_{RED} / R_{NIR} + R_{RED} + 0.16) * (1 + 0.16)$	Rondeaux et al. (1996)
Modified Chlorophyll Absorption in Reflectance Index (MCARI)	$[(R_{NIR} - R_{RED}) - 0.2(R_{NIR} + R_{GREEN})] * (R_{NIR} /R_{RED})$	Daughtry et al. (2000)
MCARI/OSAVI	MCARI/OSAVI	Daughtry et al. (2000)
Simple Ratio Index (SR)	(R_{NIR} / R_{RED})	Jordan (1969)
Modified Simple Ratio Index (MSR)	$[(R_{NIR} / R_{RED}) - 1] / [(R_{NIR} / R_{RED}) -1]^{1/2}$	Chen (1996)
Crust Index (CI)	$1 - (R_{RED} - R_{BLUE})/(R_{RED} - R_{BLUE})$	Karnieli, 1997
Biological Soil Crust Index (BSCI)	$\frac{1 - 2 \times \lvert R_{RED} - R_{GREEN} \rvert}{R_{GRNIR}^{mean}}$	Chen et al. (2005)

7 **Table S2 (Continuation)**

Index	Formulation	Reference
	Others	
$MCARI_{[705,750]}$	$[(R_{750} - R_{705}) - 0.2(R_{750} - R_{550})] * (R_{750}/R_{705})$	Wu et al. (2008)
Blog 1/R737	the first derivative of logarithm $1/R_{737}$	Yoder and Pettigrew-Crosby (1995)
DD	$(R_{749} - R_{720})/(R_{701} - R_{672})$	le Maire et al. (2004)
SIPI (Structure Insensitive Pigment Index)	$(R_{800} - R_{445})/(R_{800} - R_{680})$	Peñuelas et al. (1995)
Vogelman2	$(R_{734} - R_{747})/(R_{715} + 726)$	Vogelman et al. (1993)
PRI (Photochemical reflectance index) * Ci (chlorophyll ratio index)	$[(R_{570} - R_{530})/(R_{570} + R_{530})] * [(R_{760}/R_{700}) - 1]$	Garrity et al., (2011)
DFDS_ICCW	sum of $\rho_{675\text{-}680}$ − sum of $\rho_{640\text{-}674}$	Zhang et al. (2014)

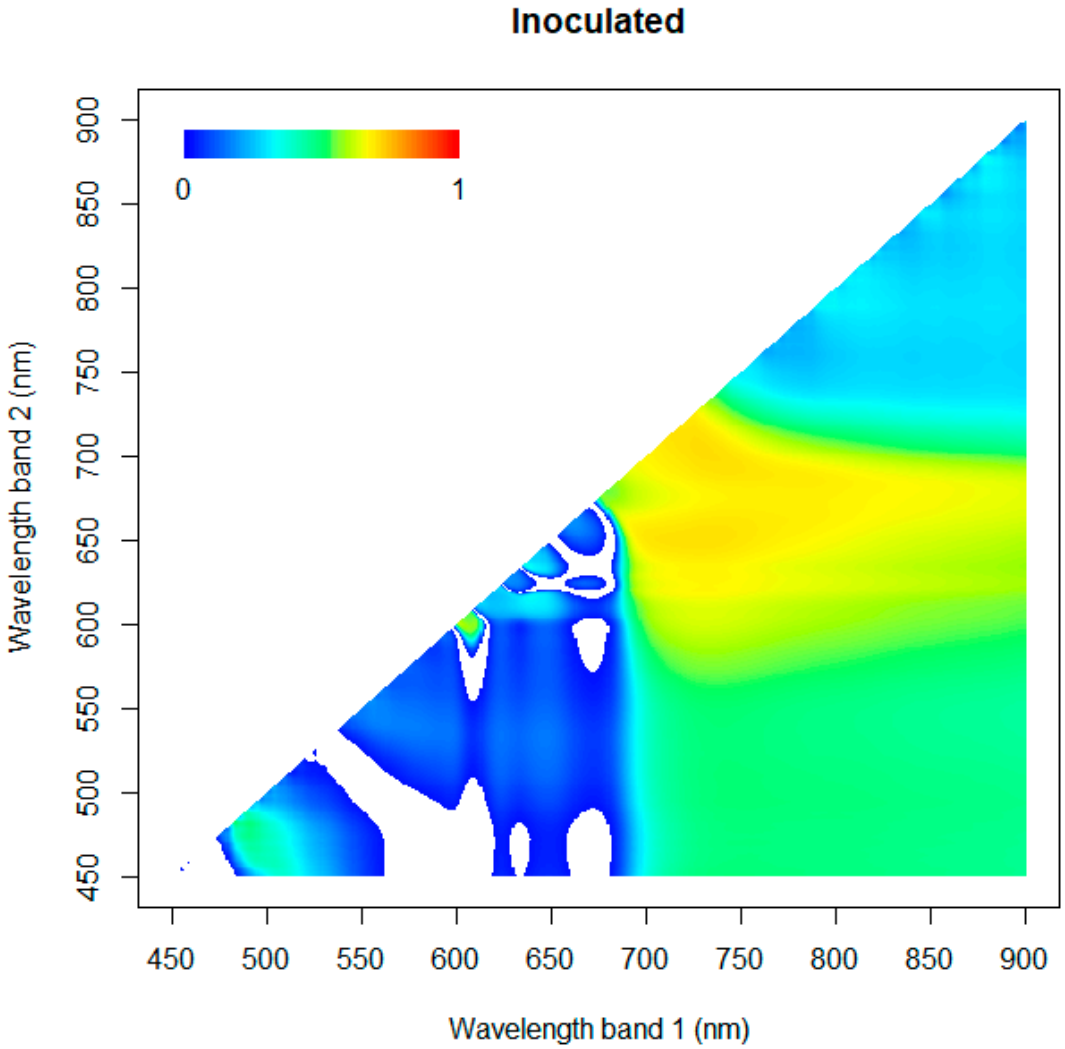

Figure S1. 2-D correlation plot illustrating the coefficient of determination (R^2) of the normalised difference indices for all possible band combinations between 450 – 900 nm at hyperspectral resolution, for cyanobacteria artificially inoculated. Only the significant values ($P < 0.05$) are represented.

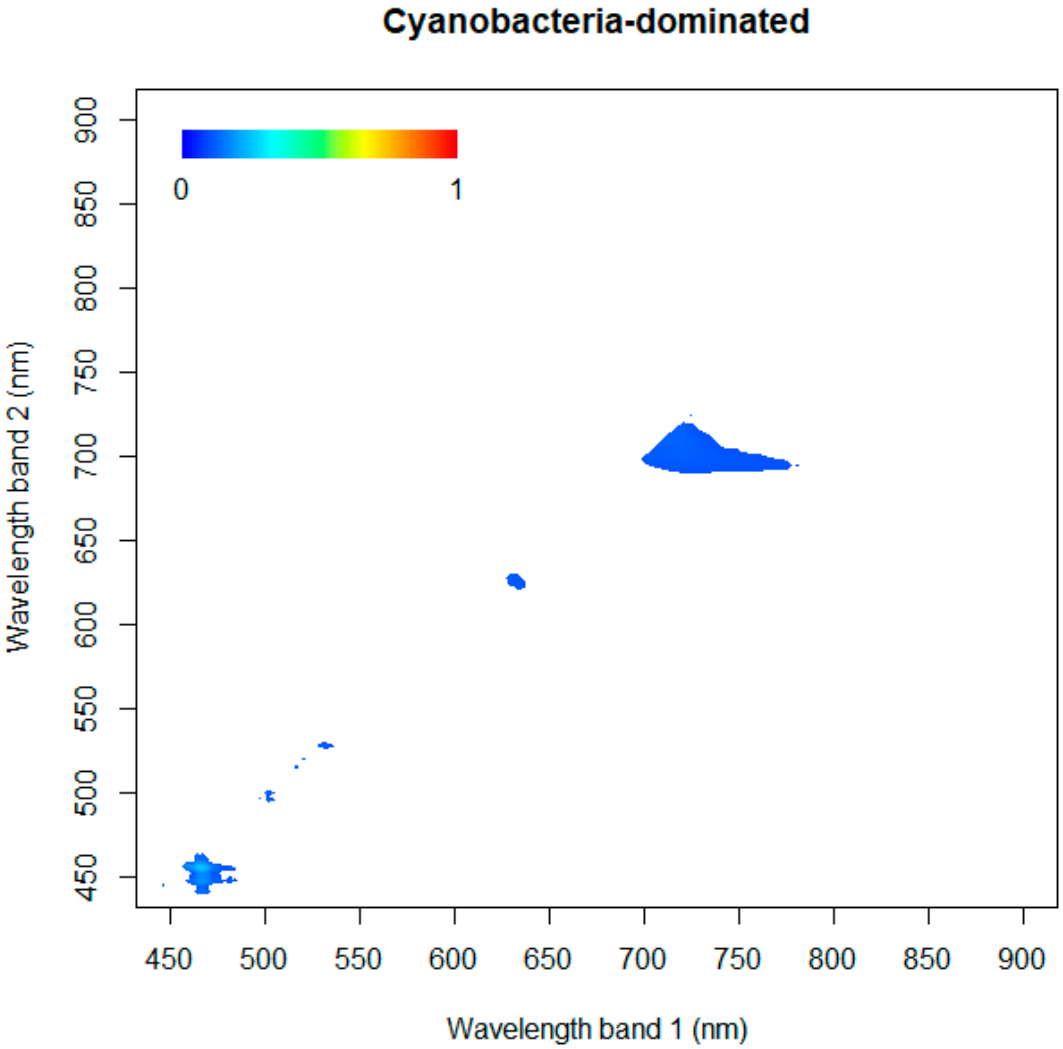

Figure S2. 2-D correlation plot illustrating the coefficient of determination (R^2) of the normalised difference indices for all possible band combinations between 450 – 900 nm at hyperspectral resolution, for natural cyanobacteria-dominated subsamples. Only the significant values ($P < 0.05$) are represented.

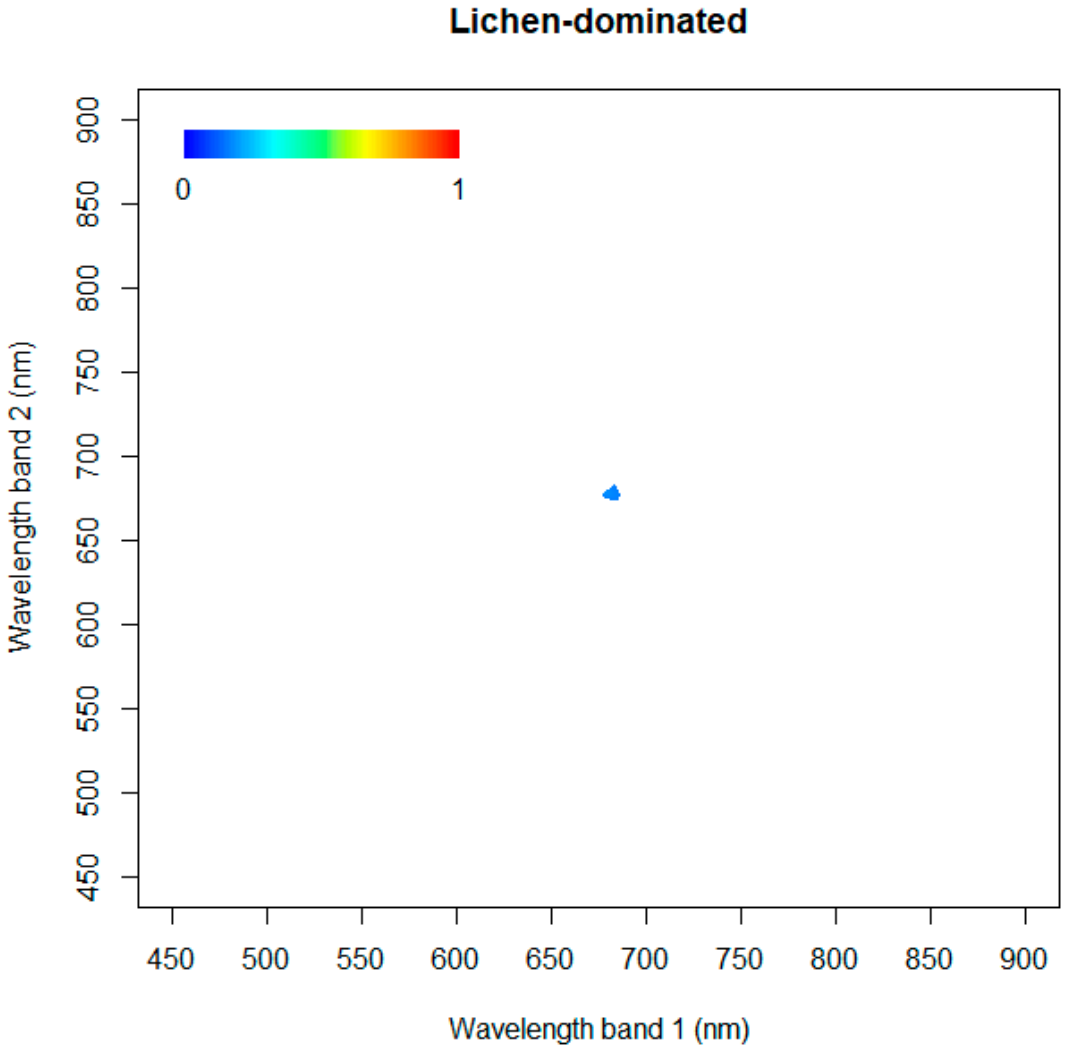

Figure S3. 2-D correlation plot illustrating the coefficient of determination (R^2) of the normalised difference indices for all possible band combinations between 450 – 900 nm at hyperspectral resolution, for natural lichen-dominated subsamples. Only the significant values ($P < 0.05$) are represented.

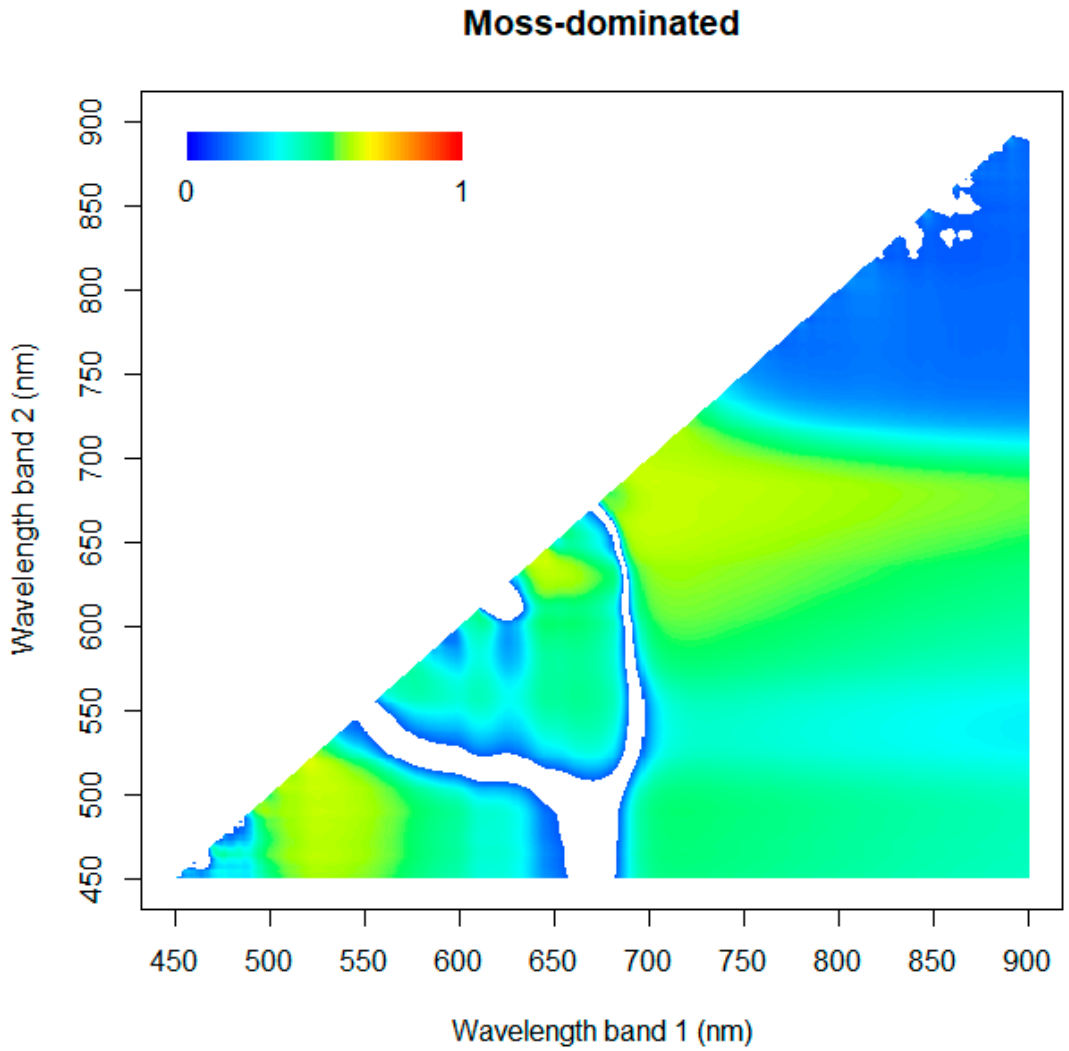

21

22 **Figure S4.** 2-D correlation plot illustrating the coefficient of determination (R^2) of the normalised
23 difference indices for all possible band combinations between 450 – 900 nm at hyperspectral resolution, for
24 moss-dominated subsamples. Only the significant values ($P < 0.05$) are represented.

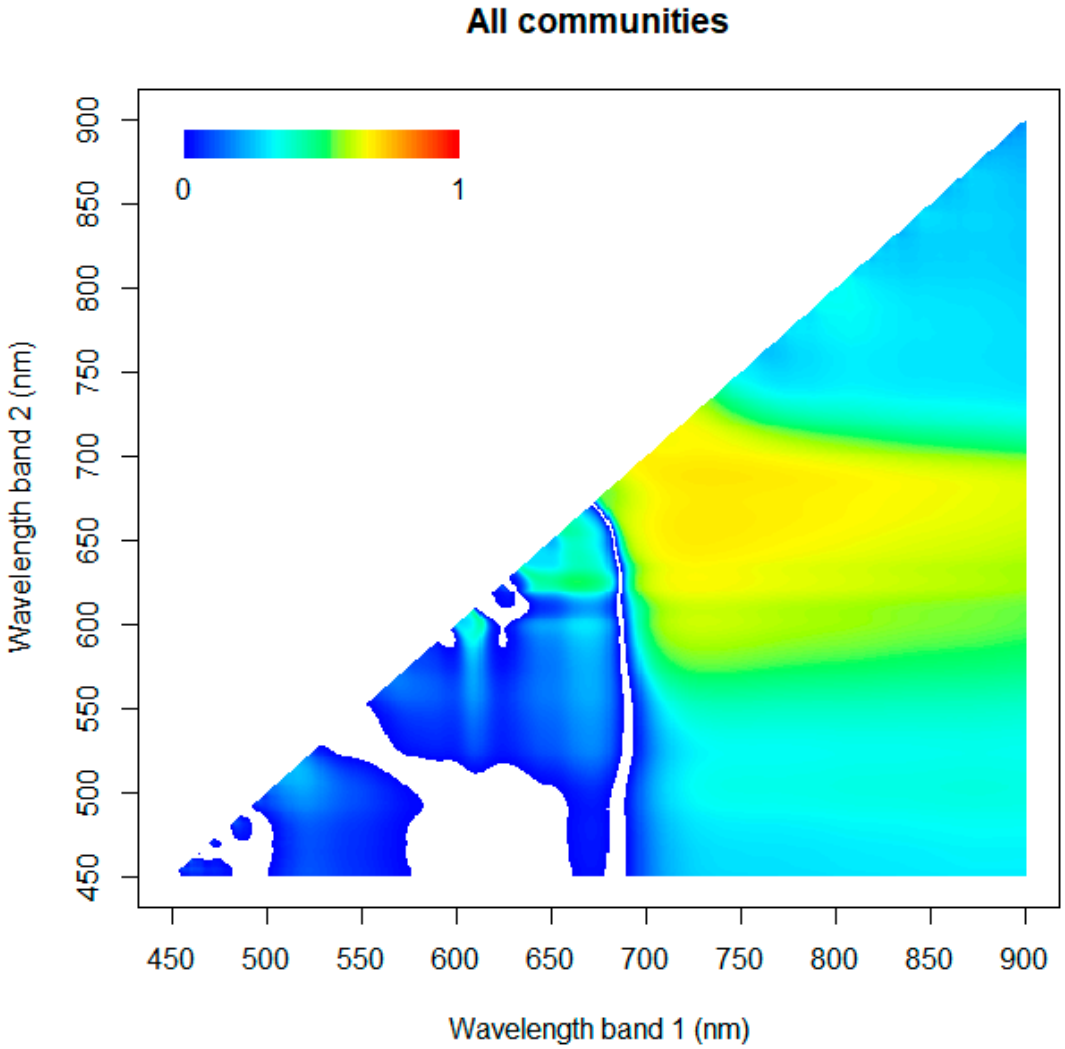

Figure S5. 2-D correlation plot illustrating the coefficient of determination (R^2) of the normalised difference indices for all possible band combinations between 450 – 900 nm at hyperspectral resolution, for the entire dataset. Only the significant values ($P < 0.05$) are represented.

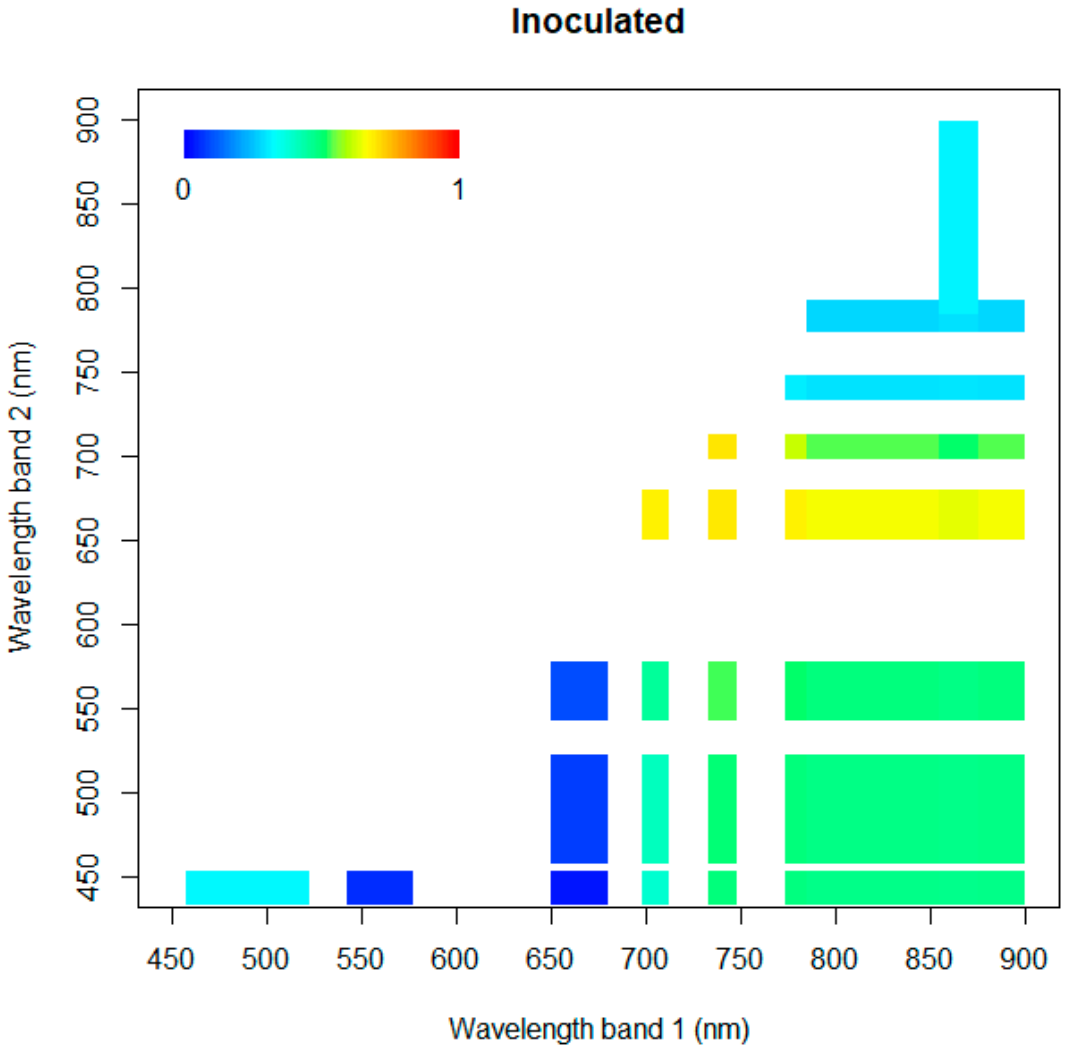

Figure S6. 2-D correlation plot illustrating the coefficient of determination (R^2) of the normalised difference indices for all possible band combinations between 450 – 900 nm at Sentinel-2 spectral resolution, for artificially inoculated cyanobacteria subsamples. Only the significant values are represented ($P < 0.05$).

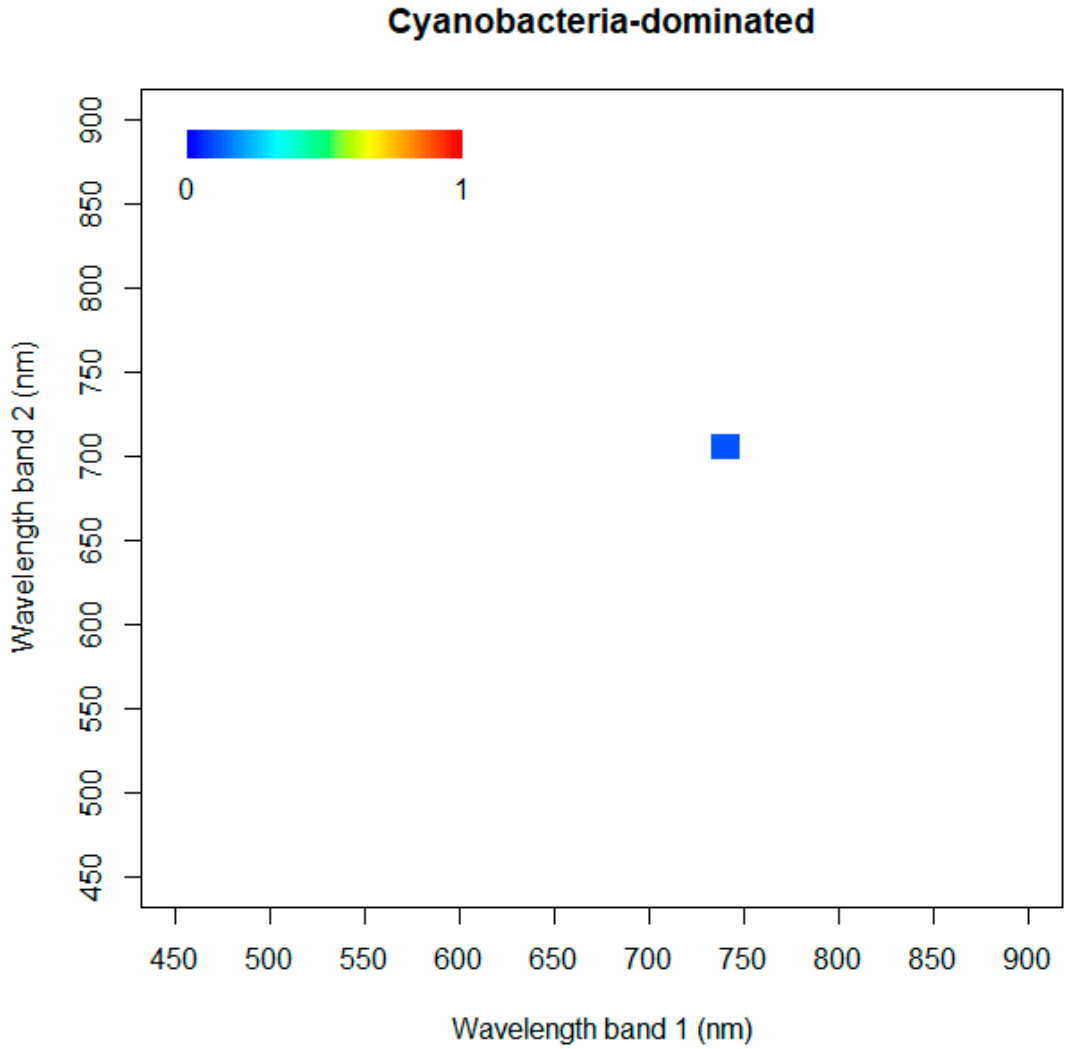

Figure S7. 2-D correlation plot illustrating the coefficient of determination (R^2) of the normalised difference indices for all possible band combinations between 450 – 900 nm at Sentinel-2 spectral resolution, for natural cyanobacteria-dominated subsamples. Only the significant values ($P < 0.05$) are represented.

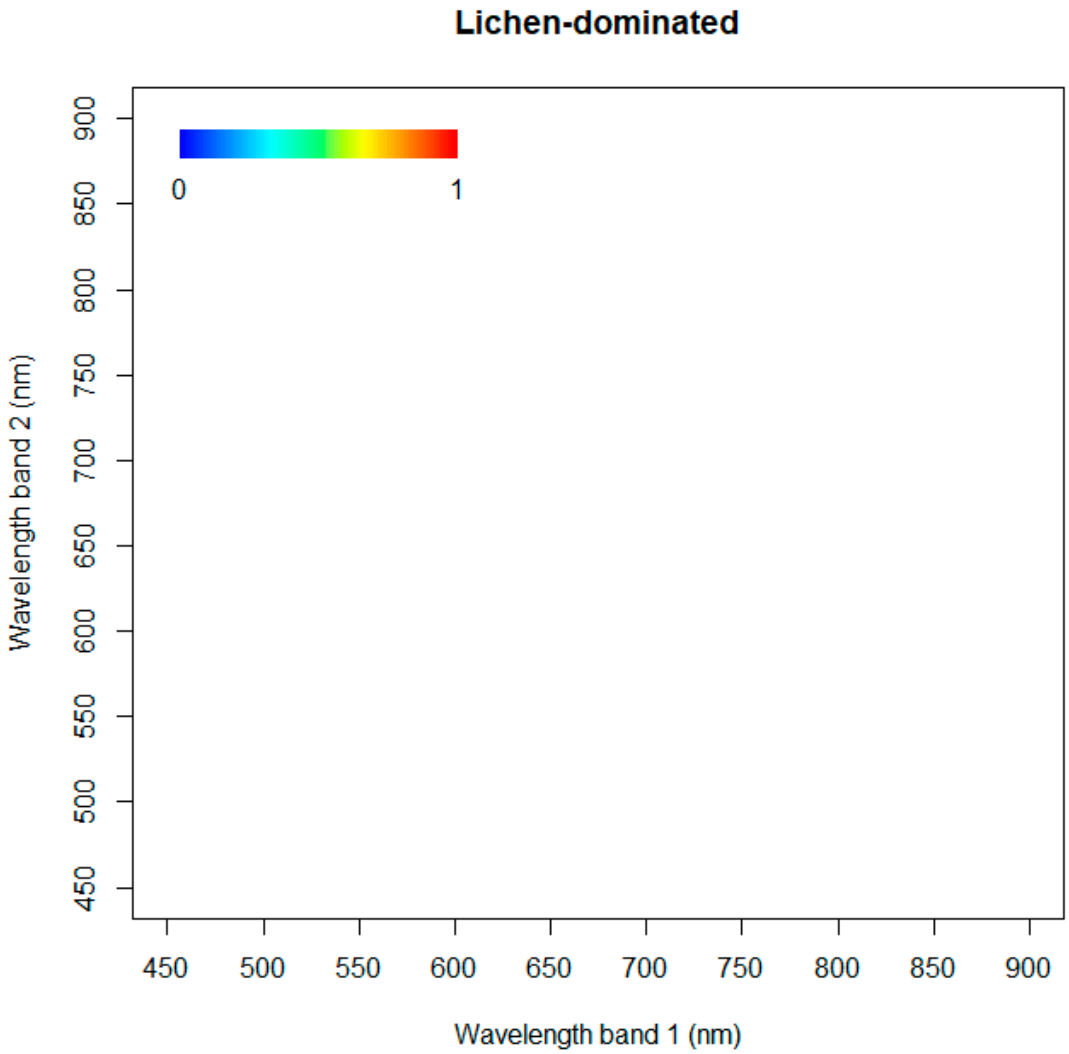

Figure S8. 2-D correlation plot illustrating the coefficient of determination (R^2) of the normalised difference indices for all possible band combinations between 450 – 900 nm at Sentinel-2 spectral resolution, for lichen-dominated subsamples. Only the significant values ($P < 0.05$) are represented.

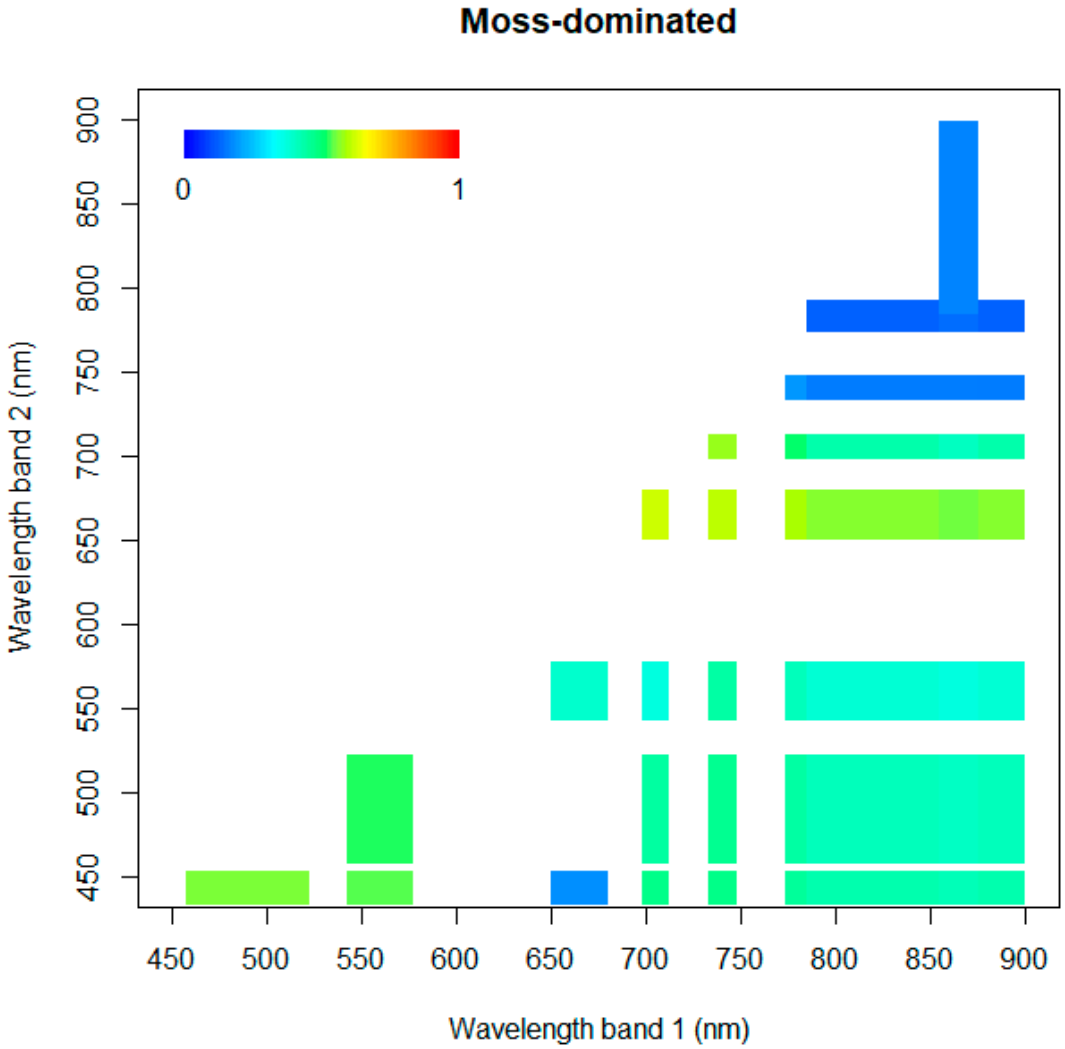

43

44 **Figure S9.** 2-D correlation plot illustrating the coefficient of determination (R^2) of the normalised
45 difference indices for all possible band combinations between 450 – 900 nm at Sentinel-2 spectral
46 resolution, for moss-dominated subsamples. Only the significant values ($P < 0.05$) are represented.

47

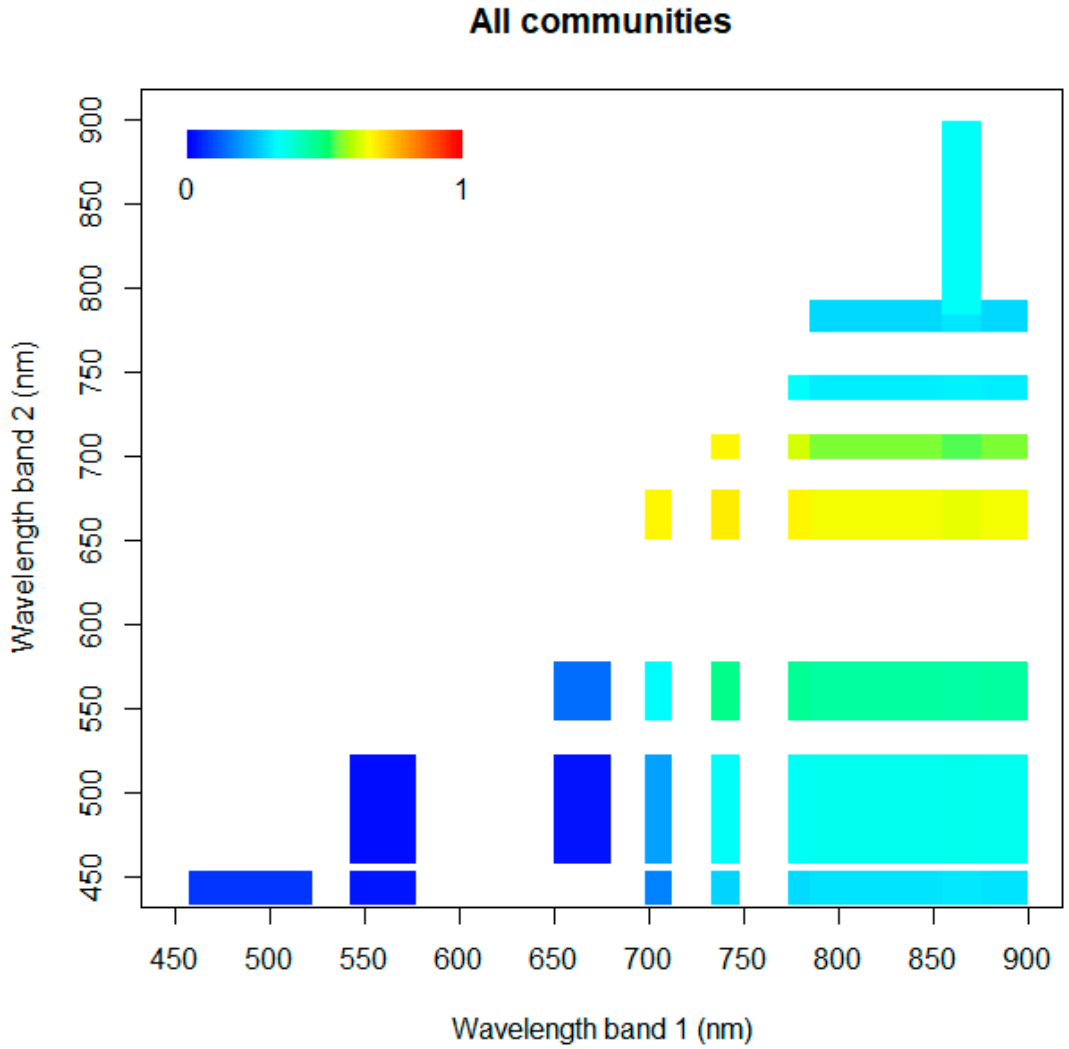

Figure S10. 2-D correlation plot illustrating the coefficient of determination (R^2) of the normalised difference indices for all possible band combinations between 450 – 900 nm at Sentinel-2 spectral resolution for the entire dataset. Only significant values ($P < 0.05$) are represented.

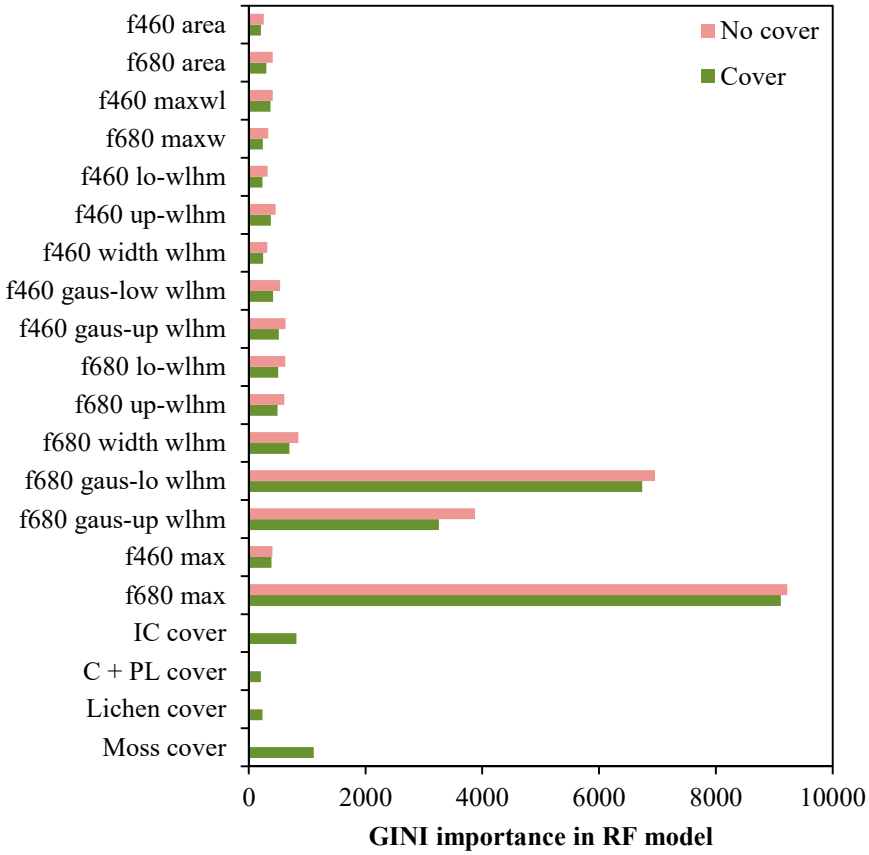

Figure S11. GINI importance of each variable in Random Forest model. Two options were tested: a) with cover (green bars) and, b) without cover (pink bars). IC: Incipient cyanobacteria, C + PL: mix of cyanobacteria and pioneer lichens.

Supplementary references

Chen, J.M., 1996. Evaluation of vegetation indices and a modified simple ratio for boreal applications. Can. J. Remote Sens. 22, 229–242. https://doi.org/10.1080/07038992.1996.10855178

Chen, J., Ming, Y.Z., Wang, L., Shimazaki, H., Tamura, M., 2005. A new index for mapping lichen-dominated biological soil crusts in desert areas. Remote Sens. Environ. 96, 165–175. https://doi.org/10.1016/j.rse.2005.02.011

Datt, B., 1998. Remote sensing of chlorophyll a, chlorophyll b, chlorophyll a+b, and total carotenoid content in eucalyptus leaves. Remote Sens. Environ. 66, 111–121. https://doi.org/10.1016/S0034-4257(98)00046-7

Daughtry, C.S.T., Walthall, C.L., Kim, M.S., De Colstoun, E.B., McMurtrey, J.E., 2000. Estimating corn leaf chlorophyll concentration from leaf and canopy reflectance. Remote Sens. Environ. 74, 229–239. https://doi.org/10.1016/S0034-4257(00)00113-9

Filella, I., Peñuelas, J., 1994. The red edge position and shape as indicators of plant chlorophyll content, biomass and hydric status. Int. J. Remote Sens. 15, 1459–1470. https://doi.org/10.1080/01431169408954177

Garrity, S.R., Eitel, J.U.H., Vierling, L.A., 2011. Disentangling the relationships between plant pigments and the photochemical reflectance index reveals a new approach for remote estimation of carotenoid content. Remote Sens. Environ. 115, 628–635. https://doi.org/10.1016/j.rse.2010.10.007

Huete, A.R., 1988. A soil-adjusted vegetation index (SAVI). Remote Sens. Environ. 25, 295–309. https://doi.org/10.1016/0034-4257(88)90106-X

Huete, A., Didan, K., Miura, T., Rodriguez, E.P., Gao, X., Ferreira, L.G., 2002. Overview of the radiometric and biophysical performance of the MODIS vegetation indices. Remote Sens. Environ. 83, 195–213.

Jordan, C.F., 1969. Derivation of Leaf-Area Index from Quality of Light on the Forest Floor. Ecology 50, 663–666. https://doi.org/10.2307/1936256

Karnieli, A., 1997. Development and implementation of spectral crust index over dune sands. Int. J. Remote Sens. 18, 1207–1220. https://doi.org/10.1080/014311697218368

Kochubey, S.M., Kazantsev, T.A., 2007. Changes in the first derivatives of leaf reflectance spectra of various plants induced by variations of chlorophyll content. J. Plant Physiol. 164, 1648–1655. https://doi.org/10.1016/j.jplph.2006.11.007

Le Maire, G., François, C., Dufrêne, E., 2004. Towards universal broad leaf chlorophyll indices using PROSPECT simulated database and hyperspectral reflectance

94 measurements. Remote Sens. Environ. 89, 1–28.
95 https://doi.org/10.1016/j.rse.2003.09.004

96 Merzlyak, M.N., Gitelson, A.A., Chivkunova, O.B., Rakitin, V.Y., 1999. Non-destructive
97 optical detection of pigment changes during leaf senescence and fruit ripening.
98 Physiol. Plant. 106, 135–141. https://doi.org/10.1034/j.1399-3054.1999.106119.x

99 Penuelas, J., Filella, I., Baret, F., 1995. Semi-empirical indices to assess
100 carotenoids/chlorophyll a ratio from leaf spectral reflectance. Photosynthetica 31,
101 221–230.

102 Peñuelas, J., Gamon, J.A., Fredeen, A.L., Merino, J., Field, C.B., 1994. Reflectance
103 indices associated with physiological changes in nitrogen- and water-limited
104 sunflower leaves. Remote Sens. Environ. 48, 135–146. https://doi.org/10.1016/0034-
105 4257(94)90136-8

106 Román, J.R., Roncero-Ramos, B., Chamizo, S. Rodríguez-Caballero, E. Cantón, Y., 2018.
107 Restoring soil functions by means of cyanobacteria inoculation: Importance of soil
108 conditions and species selection. L. Degrad. Dev. 29, 3184–3193.

109 Rondeaux, G., Steven, M., Baret, F., 1996. Optimization of soil-adjusted vegetation
110 indices. Remote Sens. Environ. 55, 95–107. https://doi.org/10.1016/0034-
111 4257(95)00186-7

112 Rouse, J.W., Haas, R.H., Schell, J.A., Deering, D.W., Harlan, J.C., 1974. Monitoring the
113 vernal advancements and retrogradation of natural vegetation. In: NASA/GSFC,
114 Final Report, Greenbelt, MD, USA, 1–137.

115 Schlemmer, M.R., Francis, D.D., Shanahan, J.F., Schepers, J.S., 2005. Remotely
116 measuring chlorophyll content in corn leaves with differing nitrogen levels and
117 relative water content. Agron. J. 97, 106–112.
118 https://doi.org/10.2134/agronj2005.0106

119 Sims, D.A., Gamon, J.A., 2002. Relationships between leaf pigment content and spectral
120 reflectance across a wide range of species, leaf structures and developmental
121 stages. Remote Sens. Environ. 81, 337–354. https://doi.org/10.1016/S0034-
122 4257(02)00010-X

123 Vogelmann, J.E., Rock, B.N., Moss, D.M., 1993. Red edge spectral measurements from
124 sugar maple leaves. Int. J. Remote Sens. 14, 1563–1575.
125 https://doi.org/10.1080/01431169308953986

126 Wu, C., Niu, Z., Tang, Q., Huang, W., 2008. Estimating chlorophyll content from
127 hyperspectral vegetation indices: Modeling and validation. Agric. For. Meteorol.
128 148, 1230–1241. https://doi.org/10.1016/j.agrformet.2008.03.005

Xue, L., Yang, L., 2009. Deriving leaf chlorophyll content of green-leafy vegetables from hyperspectral reflectance. ISPRS J. Photogramm. Remote Sens. 64, 97–106. https://doi.org/10.1016/j.isprsjprs.2008.06.002

Yoder, B.J., Pettigrew-Crosby, R.E., 1995. Predicting nitrogen and chlorophyll content and concentrations from reflectance spectra (400-2500 nm) at leaf and canopy scales. Remote Sens. Environ. 53, 199–211. https://doi.org/10.1016/0034-4257(95)00135-N

Zarco-Tejada, P.J., Miller, J.R., Mohammed, G.H., Noland, T.L., Sampson, P.H., 2002. Vegetation Stress Detection through Chlorophyll + Estimation and Fluorescence Effects on Hyperspectral Imagery. J. Environ. Qual. 31, 1433. https://doi.org/10.2134/jeq2002.1433

Zhang, J., Huang, W., Zhou, Q., 2014. Reflectance variation within the in-chlorophyll centre waveband for robust retrieval of leaf chlorophyll content. PLoS One 9. https://doi.org/10.1371/journal.pone.0110812